

## A study of EAS cores detected by the hybrid experiment at Mt.Chacaltaya

H.AOKI<sup>1</sup>, K.HONDA<sup>2</sup>, N.INOUE<sup>3</sup>, N.KAWASUMI<sup>4</sup>, N.MARTINIC<sup>5</sup>, N.OCHI<sup>6</sup>, N.OHMORI<sup>7</sup>, A.OHSAWA<sup>8</sup>,  
H.SEMBA<sup>9</sup>, M.TAMADA<sup>10</sup>, R.TICONA<sup>5</sup>

<sup>1</sup> Faculty of Science, Soka University, Hachioji, Tokyo, Japan

<sup>2</sup> Faculty of Engineering, University of Yamanashi, Kofu, Japan

<sup>3</sup> Faculty of Science, Saitama University, Saitama, Japan

<sup>4</sup> Faculty of Education, University of Yamanashi, Kofu, Japan

<sup>5</sup> Insitute de Investigaciones Fisicas, Universidad Mayor de San Andres, La Paz, Bolivia

<sup>6</sup> General Education, Yonago National College of Technology, Yonago, Japan

<sup>7</sup> Faculty of Science, Kochi University, Kochi, Japan

<sup>8</sup> Institute for Cosmic Ray Research, University of Tokyo, Kashiwa, Japan

<sup>9</sup> Faculty of Comprehensive Welfare, Urawa University, Urawa, Japan

<sup>10</sup> Faculty of Science and Engineering, Kinki University, Higashi-Osaka, Japan

tamada@ele.kindai.ac.jp

**Abstract:** Correlations among three components in the air-showers, i.e., air-shower size, burst-size and accompanied family energy, observed by Chacaltaya hybrid experiment, are studied by comparing those of simulated data. Burst-density in each block of hadron calorimeters, located at the center of air-shower array, are newly calculated using the GEANT4 simulation code in order to compare directly to the experimental data. Air-shower size is also recalculated using EGS4 in the CORSIKA package and also taking into accounts contributions of scintillator response of gamma-ray component in the air-shower. It is shown no model can describe well observed correlations between burst-size and family energy. The burst-density of the events accompanied by atmospheric family is systematically larger than expectation and also the observed family energy accompanied by the air-showers with larger burst-size is systematically smaller than that expected in the simulated events. Effects of a fluctuation in the cross-section of hadronic interactions are studied to settle the disagreement between experimental data and simulations. Inclusion of the fluctuation of the cross-section makes less attenuation of energy flow of the hadronic component in the air-shower and explains some characteristics of the experimental data.

**Keywords:** air-shower, burst, gamma-family, mountain experiment

### 1 Introduction

The hybrid experiment, operating simultaneously an air-shower array, a hadron calorimeter and an emulsion chamber at Mt. Chacaltaya (5200m, Bolivia)[1, 2], have been shown that the characteristics of the observed air-shower events in the energy region  $10^{15} \sim 10^{17}$  eV can not be fully explained simply by changing chemical composition of primary particles. In the hybrid experiments, we can obtain air-shower size,  $N_e$ , from the air-shower array data, particle-density,  $n_b$ , which are closely connected to the hadron component in the air-shower, from hadron calorimeter (burst detector) and the energy and geometrical position of individual high energy electromagnetic particles of atmospheric families by the emulsion chamber. Correlations between air-showers and accompanying families were studied by comparing experimental and simulated data using Chacaltaya data [3, 4] together with the data of the other two hybrid experiments, Tibet ASy (Yang-bajing, 4300m, China)[5, 6] and Tien-Shan (3340m, Kazakhstan)[7]. Although details of the experimental procedure are different in these hybrid experiments the results are found to be almost the same[4]. In the papers[8, 9] we have also shown some results on the correlation between burst-density and accompanied family energy observed by the Chacaltaya hybrid experiment. It is found that the experimental data are not well explained by the current model calculations. In the previous analysis, air-shower size

was estimated simply by using NKG option in CORSIKA simulation. Here, we recalculated air-shower size by using EGS4 of electromagnetic cascade and also burst-density taking into accounts the detection response of the experiment, based on the GEANT4 simulation[10].

### 2 Hybrid experiment at Mt.Chacaltaya

The air-shower array covers a circular area within a radius about 50 m by 35 plastic scintillation detectors to measure the lateral distribution of electron density of the air-showers. In the center of the air-shower array, 32 blocks of emulsion chambers (0.25 m<sup>2</sup> each) are installed. Each block of the emulsion chamber consists of 30 lead plates each of 0.5 cm thick and 14 sensitive layers of X-ray film which are inserted after every 1 cm lead. The total area of the emulsion chambers is 8 m<sup>2</sup>. Hadron calorimeters with plastic scintillator of 5cm thick are installed underneath the respective blocks of the emulsion chamber. A 2 cm thick iron support is inserted between the emulsion chamber and the hadron calorimeter. Details of the Chacaltaya hybrid experiment are described in Refs.[1, 2]

### 3 Simulations

#### 3.1 Air-shower size

For generating extensive air-showers and families we use the CORSIKA simulation code (version 6.980) [11] employing the QGSJET model (QGSJET01c)[12] for the cosmic-ray nuclear interaction. Primary particles of  $E_0 \geq 10^{15}$  eV are sampled respectively from the power law energy spectrum of integral power index  $-1.8$ , for pure protons and pure irons, and also from the energy spectrum of primary cosmic rays with proton dominant (PD) and heavy dominant (HD) chemical composition. The thinning energy in the calculations in the air-showers is fixed to be 10 GeV. Shower size,  $N_e$ , at the observation level is calculated taking into accounts detector response of low energy electromagnetic particles. The shower size increases by 25% compared with the previous calculations[8, 9] using NKG option. The increase of shower size is mainly due to the contribution of scintillator response from low energy gamma-rays, because gamma-rays also give some energy deposit in the scintillator by electromagnetic interactions. Here we use default values in the CORSIKA code for the low energy cut-off of hadrons and muons, i.e.,  $E_{cut} = 0.3$  GeV but we use  $E_{cut} = 0.001$  GeV for electromagnetic particles. Air-shower center is randomly sampled within a area of  $\pm 2.5$  m in X and Y direction from the center of 32 hadron calorimeters.

#### 3.2 High energy showers in the atmospheric families

For high energy ( $e, \gamma$ )-particles and hadrons of  $E \geq 1$  TeV in the atmospheric families arriving at each emulsion chamber, we calculate further nuclear and electromagnetic cascade development inside the chamber taking into account the exact structure of the emulsion chamber. We use a code formulated by Okamoto and Shibata for high energy electromagnetic cascade[13]. The electron number density under every 1 cmPb is converted into spot darkness of the X-ray film. Then the energy of each shower is re-estimated from the shower transition on spot darkness by applying the procedure used in the experiments.

#### 3.3 Calculation of the burst-density

Hadron calorimeters detect a bundle of charged particles, which are produced in the emulsion chamber material mainly by the hadron component in the air-shower through the local nuclear interactions. We use GEANT4 code[10] with QGSP model for hadronic interactions for calculating the burst-density. We calculate nuclear and electromagnetic cascades in the emulsion chamber and the energy deposit in the 5 cm thick plastic scintillator is estimated for all the charged particles (mainly electrons and positrons) and  $\gamma$ -rays in the cascade. Actually, the energy deposit is calculated for the hadrons (pions, protons, neutrons and kaons) and also muons and  $e, \gamma$  with 5 different energies of 10 GeV, 100 GeV, 1 TeV, 10TeV and 100 TeV, and 5 different zenith tangent of arrival direction,  $\tan \theta = 0.0, 0.2, 0.4, 0.6, 0.8$ . The distribution of the energy deposit obtained by the GEANT4 simulations are approximated by numerical functions. In order to save computing time, the energy deposit is sampled from the numerical functions for every particle incident upon the emulsion chamber and is converted into a particle number using average energy loss ( $=10$ MeV) of a single muon in the 5 cm thick plastic scintillator. Finally we get the burst-density,  $n_b$ , the number of

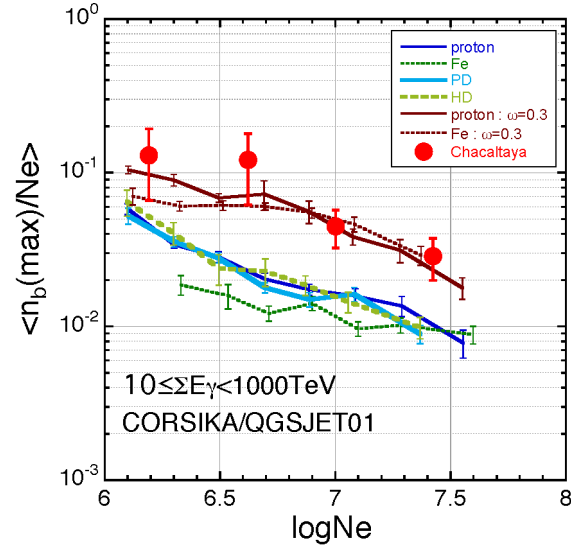


**Fig. 1:** Shower-size dependence on the maximum burst-density normalized by the accompanied air-shower size,  $n_b(max)/N_e$ . Large solid circles are for the Chacaltaya data. Lines are for the simulated events using CORSIKA with QGSJET01 model. Red lines are for the simulated events taking into accounts the effect of the cross-section fluctuation with fluctuation parameter  $\omega=0.3$ .

particles per  $0.25 \text{ m}^2$ , in each block of 32 hadron calorimeters. Details of the procedure for the calculations are given in the paper[14].

### 4 Selection of the events

We define  $n_b(max)$  as the largest burst-density among 32 blocks of hadron calorimeters. In the following we pick up the events which satisfy the following criteria;

- $N_e \geq 10^6$ ,
- $n_b(max) \geq 10^4$ ,
- $R_{AS-Bs} \leq 1 \text{ m}$ ,  
where  $R_{AS-Bs}$  is the distance between the burst center and the air-shower center,
- more than 10 among 32 blocks have burst-density  $n_b \geq 100$ .
- energy of the accompanied family is  $\Sigma E_\gamma \geq 10 \text{ TeV}$  ( $n_\gamma \geq 5$  with  $E_{min} = 2 \text{ TeV}$ ).

The burst center is determined by the algorithm described in Ref.[2]. In the Chacaltaya data 62 events are accompanied by high energy atmospheric family among 1,037 events which satisfy the above first four criteria in  $\sim 40 \text{ m}^2 \text{ year}$  exposure of hadron calorimeters. In the following, we analyze those 62 events accompanied by atmospheric families.

### 5 Characteristics of air-showers accompanied by bursts and families

#### 5.1 Air-shower size and burst size

Figure 1 shows shower-size dependence of the maximum burst-density normalized by air-shower size,  $n_b(max)/N_e$ .

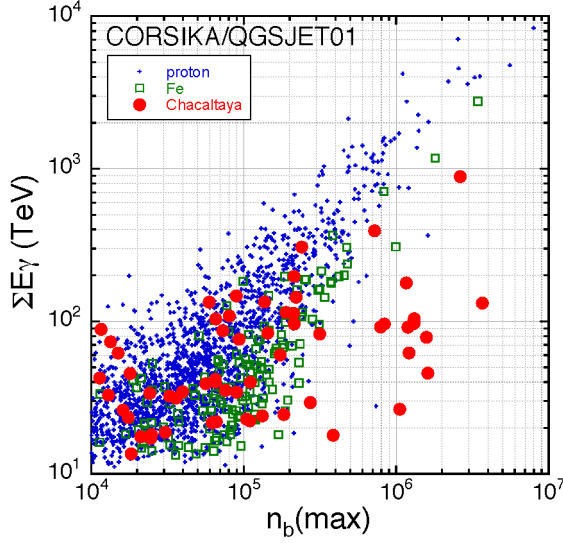


**Fig. 2:** Correlation diagram between  $n_b(max)$  and family energy  $\Sigma E_\gamma$  in the burst-triggered-families in the air-showers of  $10^6 \leq N_e < 10^8$ . Large solid circles are for the Chacaltaya data. Small dots and open squares are for proton primaries and for iron primaries, respectively, of the simulated events using CORSIKA with QGSJET01 model.

As seen in the figure, the maximum burst-density in the experimental data are systematically larger than that expected in the simulated events irrespective of the air-shower size. The distribution is almost independent of the chemical composition of primary particles though iron-primaries give a little smaller burst-density for the events with smaller air-shower size,  $N_e \leq 10^7$ .

## 5.2 Burst size and family energy

Figure 2 shows a correlation diagram between the maximum burst density  $n_b(max)$  and accompanying family energy  $\Sigma E_\gamma$ . The experimental data are compared with those of simulated data of proton- and of iron-primaries by CORSIKA/QGSJET01. As naturally expected, the family energy is roughly proportional to  $n_b(max)$  in the simulated data irrespective of the primary particles though the family energy of the events coming from iron-primaries is smaller than that from proton-primaries. We can see a lot of the experimental data are located far from the simulated events in the diagram. The family energy in the experimental data is systematically smaller than that of simulated data in the events with larger burst-density,  $n_b(max) > \sim 10^6$ .

## 6 Effect of fluctuations in hadron-Air interaction

It looks as if the fluctuation of event by event is much more in the experimental data than in simulations as seen in Figure 2. One of the possible origin of the observed large fluctuation could be due to a fluctuation in the cross-section of hadronic interaction. In the paper of Wilk and Wlodarczyk[15], non-exponential decrease of shower-starting points of the hadronic showers observed by Pamir thick lead emulsion chamber, one of the unusual phenomena in cosmic-ray interactions, was explained by introducing intrinsic fluctuations in cross-section of hadronic

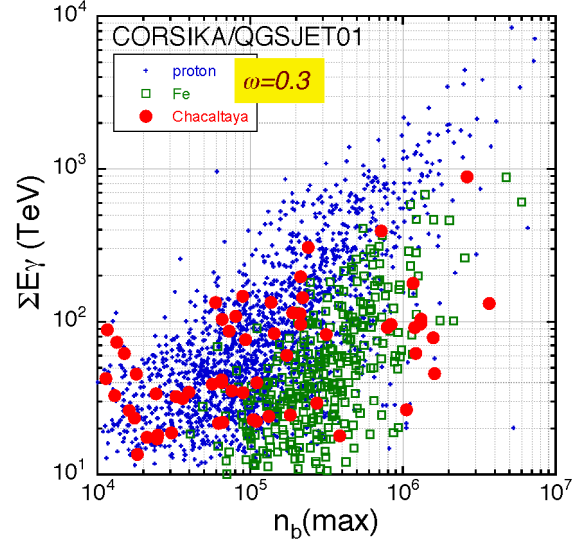


**Fig. 3:** Correlation diagram between  $n_b^{max}$  and family energy  $\Sigma E_\gamma$  in the burst-triggered-families in the air-showers of  $10^6 \leq N_e < 10^8$  in case of introducing fluctuation in the hadron-Air interaction in the simulations, with a parameter of relative fluctuation  $\omega_{N-Air}=0.3$ .

interaction[16]. Here we introduce the same fluctuation of the cross-section in high-energy hadron-air interactions and study the effect to the correlation between bursts and families observed by the hybrid experiment. We apply the same procedure used in their paper [15], that is, the cross-section,  $\sigma(E)$ , of hadron-air interaction is sampled from the uniform distribution in the interval  $[1 - \sqrt{3}\omega\sigma_0(E), 1 + \sqrt{3}\omega\sigma_0(E)]$ . Here  $\sigma_0(E)$  is the mean cross-section at the energy  $E$  and  $\omega$  is the relative fluctuation of the cross-section. We assume the parameter  $\omega_{\pi-Air}$  for meson-air interaction is 1.6 times of  $\omega_{N-Air}$  for nucleon-air interaction. We apply these modification in the CORSIKA simulation code and calculate air-showers, bursts and high energy atmospheric families. The results are shown in Figure 3 for the case of  $\omega_{N-Air} = 0.3$ . The simulated data scattered out more widely when the fluctuation of the cross-section is included in the calculations, though the frequency to observe the events with larger  $n_b(max)$  and smaller  $\Sigma E_\gamma$  at the same time is still smaller in simulations than that in the experiment. In Figure 1 we show the shower size dependence of the  $n_b(max)/N_e$  also for the simulated events including cross-section fluctuation. It is seen that the experimental data are well described by taking into accounts the fluctuation of the cross-section.

Figure 4 shows average longitudinal development of air-showers, in the form of the number of particles, for the primary protons and irons of  $E_0 = 10^{16}$  eV. Also shown are those for the case including fluctuation of the interaction cross-section. Here we put the cut-off energy is 1 MeV for  $e^+, e^-$  and 300 MeV for hadrons. The shape of shower development in the case of inclusion of the cross-section fluctuation is not much different from those without fluctuations. That is, we can not see the effect of the cross-section fluctuation in the usual air-shower observations. Figure 5 shows average longitudinal development of the air-showers in the form of the energy flow of the particles. Here we apply high energy cut-off,  $E_{cut} = 1$  TeV both for  $e^+, e^-$  and hadrons. As seen in the figure, inclusion of

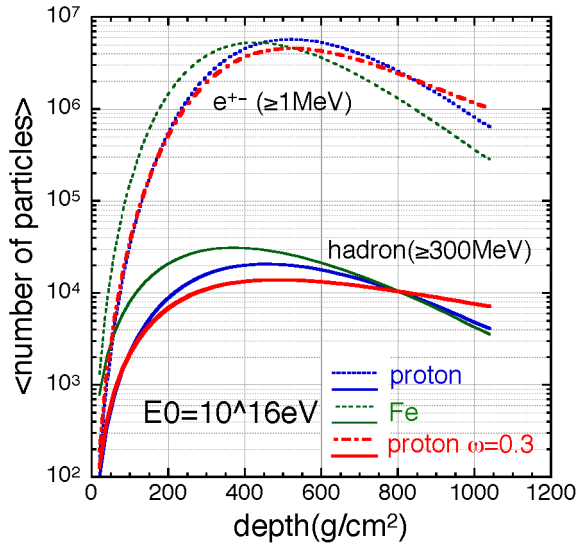


**Fig. 4:** Air-shower development in the form of the number of particles for the primary protons and irons of  $E_0 = 10^{16}$  eV. Broken lines are for  $e^+, e^-$  component with  $E_{cut} = 1$  MeV and solid lines are for the hadron component with  $E_{cut} = 300$  MeV. Red lines are for the simulated events taking into accounts the effect of the cross-section fluctuation with fluctuation parameter  $\omega_{N-Air} = 0.3$ .

the fluctuation of the cross-section makes less attenuation of energy flow, especially of the hadronic component in the air-shower. The energy flow of the hadron component at Chacaltaya altitude becomes significantly larger when the fluctuation of cross-section is taken into accounts. In contrast to the hadron component, the energy flow of  $e^+, e^-$  is almost unchanged even when the cross-section fluctuation is taken into accounts at Chacaltaya altitude. This is a reason why inclusion of the fluctuation of cross-section makes more events with larger burst density for given family energies.

## 7 Summary and discussions

The characteristics of the air-showers accompanied by burst and atmospheric family in their core are studied. The burst density in those events are considerably larger than those expected by simulated events. Also the family energy accompanied by the events with larger burst-density is considerably smaller than those of simulated events.

Some changes of the characteristics of particle production may cause the discrepancy between experimental and simulated data, but recent results of the LHCf experiment show the production spectra of secondary particles in p-p collisions at  $\sqrt{s} = 7$  TeV are not much different from those assumed in current simulation models though no model can describe well the LHCf data[17]. As an another possibility, we considered the effect of the fluctuation in the cross-section of hadron-air interactions. It is found that the disagreement between experimental and simulated data at the mountain altitude becomes smaller when the cross-section fluctuation is taken into accounts.

The air-shower events which are used in the present analysis are those accompanied by atmospheric families. The number of those events are less than 10 % of all the events with  $N_e \geq 10^6$  and  $n_b(max) \geq 10^4$  in the experimen-

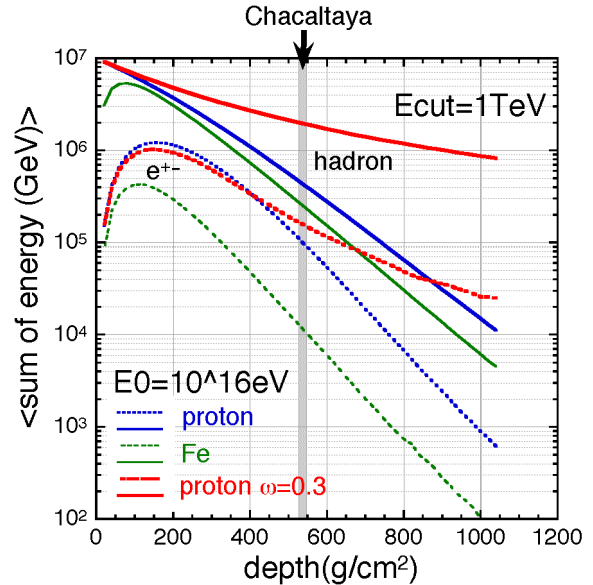


**Fig. 5:** Air-shower development in the form of energy flow of particles for the primary protons and irons of  $E_0 = 10^{16}$  eV, Cut off energy is 1 TeV for both  $e^+, e^-$  and hadron components. Symbols are same to those in Figure 4.

tal data, while 30 ~ 40 % of the events accompany atmospheric families in the simulated events.

## References

- [1] N.Kawasumi et al., Phys. Rev. D **53** (1996) 3534
- [2] C.Aguirre et al., Phys. Rev. D **62** (2000) 032003
- [3] H.Aoki et al., Proceedings of 30th ICRC, Merida (2007), Vol.4, p.23
- [4] S.P.Besshapov et al., Nucl. Phys. B (Proc. Suppl.) **196**(2009) 118; Proceedings of 31th ICRC, Lodz (2009) #0214
- [5] Tibet AS $\gamma$  Collaboration (M.Amenomori et al.), Phys. Rev. D **62** (2000) 112002-1, 072007-3
- [6] Tibet AS $\gamma$  Collaboration (M.Amenomori et al.), Phys. Lett. B **632** (2006) 58
- [7] S.B.Shaulov, AIP Conf. Proc. **276** (1992) 94
- [8] M.Tamada, Proc. 16th Int. Symp. on Very High Energy Cosmic Ray Interactions (2010), Fermilab eConf C1006284 (<http://www.slac.stanford.edu/econf/C1006284>) C27
- [9] H.Aoki et al., Proceedings of 32th ICRC, Beijing (2011) Vol.1, p205
- [10] S.Agostinelli et al. Geant4 collaboration, Nucl. Inst. and Meth. A **506**(2003) 250
- [11] D.Heck, J.Knapp, J.N.Capdevielle, G.Schatz and T.Thouw, Fortshungzentrum Karlsruhe, FZKA 6019 (1998)
- [12] N.N.Kalmykov and S.S.Ostapchenko, Yad. Fiz. **56** (1993) 105
- [13] M.Okamoto and T.Shibata, Nucl. Instr. and Meth. A **257** (1987) 155
- [14] T.Yamasaki and M.Tamada, Proceedings of 32th ICRC, Beijing (2011) Vol.1, p216
- [15] G.Wilk and Z.Wlodarczyk, Phys. Rev. D**50** (1994) 2318
- [16] B.Blättel et al., Phys. Rev. D**47** (1993) 2761
- [17] O.Adriani et al. ( LHCf Collaboration), Phys. Lett. B**703** (2011) 128